JOURNAL OF SYNCHROTRON RADIATION

ISSN 1600-5775

Concentrated protein solutions investigated using acoustic levitation and small-angle X-ray scattering

Pernille Sønderby,[a] Christopher Söderberg,[b]‡ Christian G. Frankær,[c] Günther Peters,[a] Jens T. Bukrinski,[d] Ana Labrador,[b] Tomás S. Plivelic[b] and Pernille Harris[a]*

[a]Department of Chemistry, Technical University of Denmark, Kemitorvet B207, DK-2800 Kgs Lyngby, Denmark, [b]MAX IV Laboratory, Lund University, PO Box 118, 221 00 Lund, Sweden, [c]Deparment of Chemistry, University of Copenhagen, Universitetsparken 5, DK-2100 Copenhagen, Denmark, and [d]CMC Assist Aps, DK-2500 Copenhagen, Denmark. *Correspondence e-mail: ph@kemi.dtu.dk

Received 22 March 2019
Accepted 19 December 2019

Edited by M. Yamamoto, RIKEN SPring-8 Center, Japan

‡ Present address: RISE Research Intitutes of Sweden, Division of Bioscience and Materials, Box 5607, SE-114 86 Stockholm, Sweden.

Keywords: SAXS; levitated droplet; concentrated protein solutions; structure factors.

Supporting information: this article has supporting information at journals.iucr.org/s

An acoustically levitated droplet has been used to collect synchrotron SAXS data on human serum albumin protein solutions up to a protein concentration of 400 mg ml^{-1}. A careful selection of experiments allows for fast data collection of a large amount of data, spanning a protein concentration/solvent concentration space with limited sample consumption (down to 3 µL per experiment) and few measurements. The data analysis shows data of high quality that are reproducible and comparable with data from standard flow-through capillary-based experiments. Furthermore, using this methodology, it is possible to achieve concentrations that would not be accessible by conventional cells. The protein concentration and ionic strength parameter space diagram may be covered easily and the amount of protein sample is significantly reduced (by a factor of 100 in this work). Used in routine measurements, the benefits in terms of protein cost and time spent are very significant.

1. Introduction

Proteins are increasingly used in the pharmaceutical industry as biologics or as industrial enzymes in catalysis or in food and feed technology as a bio-sustainable supplement for the chemical industry. One of the major challenges in handling proteins is their tendency to aggregate, which becomes an even bigger issue as it is often preferable to have the proteins in high concentrations. One example is antibodies administered in concentrations of 50–100 mg ml^{-1} when used in cancer treatments. Other examples where it is necessary to be able to stabilize proteins in very high concentrations are in production pipelines where the water consumption increases enormously if only diluted solutions of protein can be produced. Therefore, being able to stabilize and characterize proteins in high concentrations is becoming increasingly important (Saluja & Kalonia, 2008; Shire *et al.*, 2004).

It is, however, a fact that the mechanistic understanding and the tools for preventing aggregation in high-concentration protein samples are lacking, mainly due to very few experiments performed at high protein concentrations (above 50 mg ml^{-1}). The aggregation of proteins can be due to non-specific effects, where steric effects force the proteins to associate, but can also be due to more specific effects such as hydrophobic patches on the surface that make the protein partly unfold. Furthermore, the tendency to aggregate depends on the buffer. Parameters like pH, ionic strength,

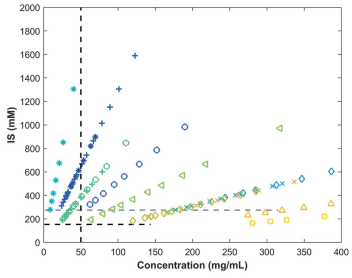

Table 1
Human serum albumin formulations used in this study.

Constituents	pH	Ionic strength
145 m*M* NaCl, 8 m*M* octanoate, 0.05 mg ml^{-1} polysorbate 80	∼7.0	153 m*M*
25 m*M* NaH_2PO_4, 215 m*M* NaCl	6.5	259 m*M*

type of salt and additives like sugar affect the protein behaviour and may make the protein more or less aggregation prone. In order to be able to stabilize proteins it is necessary to have a thorough knowledge of the protein behaviour, and to characterize protein inter-mutual interactions in a given sample. This is, however, not an easy task as many of the techniques used to characterize protein structure and behaviour either fail at high concentrations (>50 mg ml^{-1}) or will consume enormous amounts of sample. Small-angle X-ray scattering (SAXS), however, is a technique that does not have any limit with respect to the sample concentration. Weak protein–protein interactions may be characterized in a given sample up to very high protein concentrations (Pellicane & Cavero, 2013; Sønderby *et al.*, 2018; Tardieu *et al.*, 1987). Using SAXS it is possible to characterize the oligomeric equilibrium of the samples as well as the weak interactions. Normally, protein SAXS is performed in a glass capillary, preferably in a flow-through cell, and the sample at very high concentrations is difficult to control. It becomes viscous and slippery, and the risk of wasting a very precious sample is enormous.

In this study we have used an acoustically levitated droplet mounted on the I911-SAXS beamline at the MAX IV Laboratory in Sweden to investigate human serum albumin at protein concentrations up to 400 mg ml^{-1}. Acoustic levitators have been used as a container-free environment (Foresti *et al.*, 2013) for particles (Xie *et al.*, 2002) and crystallization (Lü *et al.*, 2005), and have been used in combination with a variety of characterization techniques, such as fluorescence (Leiterer *et al.*, 2008*a*), SAXS (Delissen *et al.*, 2008; Leiterer *et al.*, 2008*b*) and SANS/SAXS and circular dichroism (Cristiglio *et al.*, 2017). In the latter, the scattering data analysis was qualitative and the focus was on applications within lyophilization. In a recent protein X-ray crystallography experiment (Tsujino & Tomizaki, 2016), X-ray diffraction data from lysozyme crystals in levitated droplets were collected and paved a way to collect data at room temperature at intense synchrotron beamlines.

Human serum albumin (HSA) is a well studied protein used to stabilize other proteins in drug formulations and in drug delivery systems. In a previous study we have used a combination of SAXS and static light scattering to study the solution properties and self-interaction of HSA in three different buffer systems with different ionic strengths (Sønderby *et al.*, 2018). Here we combine the acoustic levitator and small-angle X-ray scattering to investigate HSA samples at high protein concentrations and high salt concentrations. We demonstrate how to overcome the challenges with data reduction and show that, by using relatively few experiments and a minimum amount of sample, we are able to cover a wide range of the protein concentration/ionic strength parameter space. The obtained data are of high quality and comparable with standard flow cell data collected at the same beamline, showing the potential of the method as a standard analysis tool.

2. Materials and methods

2.1. Sample preparation

Recombinant human serum albumin (rHSA) in the form of Recombumin® alpha and Recombumin® elite given in Table 1 was kindly provided by Albumedix Ltd. rHSA was prepared by up-concentrations (Pall Nanosep® centrifugal device with Omega membrane 10 K cut-off, 5 ml) and afterwards diluted by run-through buffer. The run-through buffer was checked for protein content and the initial protein concentration was determined by UV-Vis spectroscopy on a NanoDrop 1000 Spectrophotometer from ThermoScientific at 280 nm using an extinction coefficient of 34445 cm^{-1} M^{-1}, calculated using *ProtParam* (Gasteiger *et al.*, 2005) from the primary sequence of HSA.

2.2. SAXS experiment with levitator

Levitation experiments were performed at the beamline I911-SAXS (Labrador *et al.*, 2013) of the MAX IV Laboratory, Lund University, as described previously by Agthe *et al.* (2016). Specifications for the SAXS setups used in this study are shown in Table S2 of the supporting information.

The levitator was an Ultrasonic levitator (Tec5 AG, Germany) operating at 100 kHz. It was placed upside-down in the hutch and mounted on an *xyz* stage for best alignment of the droplet in the X-ray beam as depicted in Fig. 1. Alignment of the beam at the centre of the droplet was performed for each experiment after droplet levitation, but not during acquisition. Convection in the droplet occurs in the acoustic levitation (Frohn & Roth, 2000; Sadek *et al.*, 2015). This ensures proper mixing of the sample during the experiment and furthermore reduces possible radiation damage. The droplet is exposed to air, and water will evaporate. Hereby both the protein and the buffer constituents in the sample are concentrated *in situ* during the experiment. The temperature at the mini-hutch was monitored during all experiments without noticing significant changes.

A Hamilton syringe (100 µL and 10 µL) or a sterile disposable syringe, 1 ml (26 GA 3/8 In, 0.45 × 10 mm, BD plasticpak™, Spain) was used to apply the protein droplet of approximate volume 2–3 µL in the acoustic field of the levitator.

The droplet size was monitored using a USB-microscope camera and its dimensions were subsequently analyzed using a MATLAB code. After converting the images to black and white, the vertical and horizontal dimensions of the droplet were measured. The volume of the droplet was then determined using the formula for an ellipsoid, $V = (4/3)\pi abc$, assuming that the horizontal dimensions were equal, *i.e.* $a = b$, as illustrated in Fig. S1 of the supporting information. The initial protein concentration and the measured volumes of the droplet were used to determine the *in situ* protein concen-

Table 2
Data collection and experimental conditions for selected rHSA samples.

The initial concentration was that of the levitated droplet, while the concentration of the droplet in the first frame in the scattering experiment is higher due to closing of the shutter and start of the experiment, causing the droplet to evaporate before data acquisition.

Initial rHSA concentration / first frame (mg ml^{-1})	Buffer	Data acquisition time / break (s)	Total exposure time (min)	No. of frames	Initial volume (µL)	Final rHSA concentration (mg ml^{-1})	Ionic strength range (m*M*)
20 / 26	145 m*M* NaCl, 8 m*M* octanoate 0.05 mg ml^{-1} Tween 80	30 / 30	12	10	2.0	111	153–50
100 / 120	145 m*M* NaCl 8 m*M* octanoate 0.05 mg ml^{-1} Tween 80	30 / 10	13.3	15	2.9	286	153–440
20 / 24	25 m*M* NaH_2PO_4 215 m*M* NaCl	10 / 50	17	15	2.3	123	259–1590
100 / 137	25 m*M* NaH_2PO_4 215 m*M* NaCl	10 / 50	12	10	3.0	284	259–735

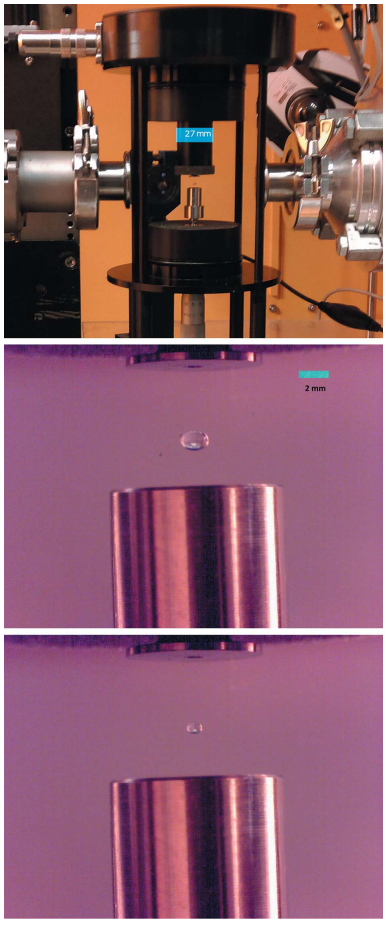

Figure 1
The levitator placed inside the mini-hutch at the I911-SAXS beamline (top). The droplet volume decreases over time due to water evaporation (middle: start point, t = 0 min; bottom: final state, t = 12 min). Blue bars: scale.

tration in the droplet. SAXS data acquisition and droplet monitoring was synchronized. Throughout the experiments, the droplet size (starting at ∼1.5 mm) was significantly larger than the beam size (0.3 mm). Data normalization according to the change of pathlength due to evaporation was performed according to the procedure described in Section 2.3; however, data with comparable droplet-to-beam size were not evaluated.

Table 2 summarizes the data collection: acquisition exposure time, delay between data acquisitions, total time of the experiment, number of frames, initial volume, protein concentration and ionic strength covered for selected data. The corresponding scattering curves are shown in Fig. S4.

2.3. SAXS data treatment

SAXS data reduction and normalization to the incident beam and sample thickness were performed using the beamline software *PyQtFAI*. For azimuthal integration, *PyQtFAI* relies on PyFAI, a library for data reduction of scattering images, developed at ESRF (Ashiotis *et al.*, 2015). Further scaling and structure factor determination was performed using *Primus* (Konarev *et al.*, 2003) from the *ATSAS* software package (Konarev *et al.*, 2006).

A brief description of the procedure used in *PyQtFAI* to account for the change in sample pathlength during the measurement (sample evaporation) is described in the following.

In *PyQtFAI* we use the following procedure for normalization, taken from Meisburger *et al.* (2013).

The transmission factor T_s of a sample is defined as

$$T_s = I_i/I_0, \tag{1}$$

where I_0 and I_i are the intensities of the incident and transmitted beam, respectively.

We measure I_0 and I_i at the same time using two different detectors; thus we use the empty 'cell' transmittance to cross-calibrate the two detectors. T is then finally calculated as

$$T = \left(\frac{I_0^E}{I_i^E}\right)\left(\frac{I_i^S}{I_0^S}\right), \tag{2}$$

where the superscripts E and S denote 'empty' and 'sample', respectively.

In our final normalization to produce $I(q)$ in equation (5) we use the intensity of the transmitted beam, I_i, the exposure time [equations (3) and (4)] and $\ln(1/T)$, where $\ln(1/T)$ is proportional to the sample pathlength according to the Beer–Lambert law,

$$\text{norm}_S = I_i^S \times \text{exposure time}_S, \quad (3)$$

$$\text{norm}_E = I_i^E \times \text{exposure time}_E, \quad (4)$$

$$I^S(q) = \left(\frac{I^S}{\text{norm}_S} - \frac{I^E}{\text{norm}_E}\right) \Big/ \ln\left(\frac{1}{T}\right). \quad (5)$$

Finally, the scattered intensity from the macromolecule, $I(q)$, is

$$I(q) = I^S(q) - I^b(q), \quad (6)$$

where I^S (intensity from sample) and I^b (intensity from buffer alone) have been normalized according to equation (5). Absolute intensity scaling for the data was performed using the scattering from milliQ water as secondary standard (Orthaber *et al.*, 2000). The accuracy of the normalization process using equation (5) is exemplified for a milliQ water droplet measurement in Fig. S2.

Form factors for rHSA were derived from previous data collected at the same beamline and using a standard flow-cell system (Sønderby *et al.*, 2018). These form factors were used to derive the structure factors for the data collected from the droplets in the levitator.

Then, the structure factor, $S(q)$, for each concentration c was derived as

$$S(q) = \frac{I(q)}{c} \Big/ P(q), \quad (7)$$

where $I(q)$ is the measured intensity and $P(q)$ is the form factor obtained from diluted protein solutions.

3. Results and discussion

In the droplet experiment the same sample is exposed to X-rays between eight and ten times for 10–30 s with waiting times of 30–50 s in between (further details are given in Table 2). Despite the multiple exposures, we did not observe radiation damage for any exposure times reported in the manuscript. The convection-driven mixing on the levitator seems to prevent radiation damage in a similar way to the effect of sample oscillation within a flow cell.

The increase in protein concentration during a levitation experiment is dependent on the initial protein concentration, the solution excipients and the volume of the droplet (Schiffter & Lee, 2007*a*,*b*). However, it is very important to guarantee the reproducibility of the evaporation profile for the same experimental conditions at the beamline. This is presented in Fig. 2. Fig. 2(*a*) shows the results from buffer measurements performed for two different droplets with similar sizes on different days. The correlation is extremely good (within the experimental error) excluding possible interference from small changes of temperature or humidity

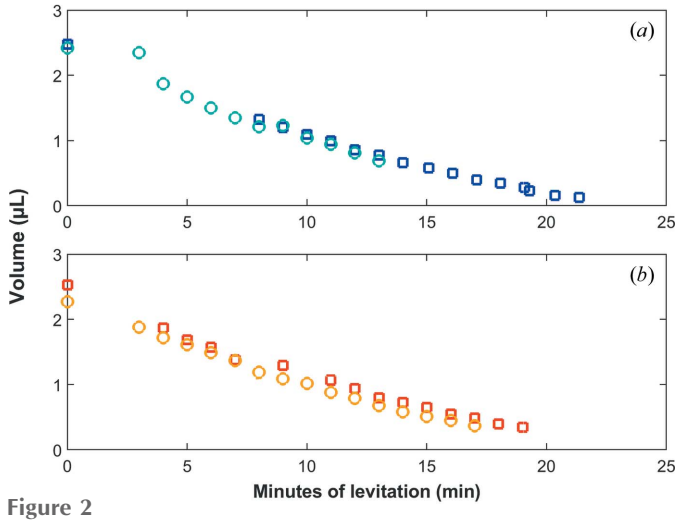

Figure 2
Evaporation of the droplets as a function of time. (*a*) 25 m*M* NaH_2PO_4, 215 m*M* NaCl buffer. Dark blue: acquisition time 30 s, delay between exposure 30 s (30/30). Light blue: 10/50. (*b*) rHSA in buffer (*a*) droplet with a start concentration of 20 mg ml^{-1}. Red: 30/30; yellow: 10/50 [data acquisition time/break (s)].

at the mini-hutch. Similar results were observed for rHSA at 20 mg ml^{-1} [Fig. 2(*b*)].

3.1. Data quality and buffer subtraction

Examples of raw data are shown in Fig. 3 for a droplet with initial concentration of 20 mg ml^{-1} rHSA in 145 m*M* NaCl, 8 m*M* octanoate and 0.05 mg ml^{-1} polysorbate 80.

The scattering from the buffer to be extracted from the sample was evaluated by comparing the ratios of the sample volume at a specific exposure with the initial sample volume, $V_r = V_{sample}/V_{initial}$. In this way we could include the concentration effect from the levitation for both the sample and the buffer. Since the evaporation rate of sample in buffer compared with buffer alone is not the same as illustrated in Fig. 2, the variable time cannot be used for buffer subtraction.

To illustrate the quality of the SAXS signals on the levitation setup, we have compared data from the same sample acquired using this setup and in the standard flow-through cell available at the beamline (with similar experimental conditions; see details in Table S2). Following Cavalcanti *et al.* (2004) and Dubuisson *et al.* (1997), the signal-to-background ratio (S/B) parameter was evaluated in both cases (see Fig. 4). S/B is defined as

$$\text{S/B}(q) = \frac{I(q)_{\text{protein}} - I(q)_{\text{Buf}}}{I(q)_{\text{Buf}}}, \quad (8)$$

where $I(q)_{\text{protein}}$ is the scattering from the protein in solution and $I(q)_{\text{Buf}}$ is the scattering from the buffer.

In Fig. 4, we present the first measurement in the 20 mg ml^{-1} droplet series as the worst-case scenario for the comparison (low concentration comparison). As expected, S/B is better for the flow cell due to the absence of long air-scattering paths (for accommodating the levitator) and plastic-based windows on the evacuated chambers, especially in the q-range below 0.07 Å^{-1}. The ratio between the sample scat-

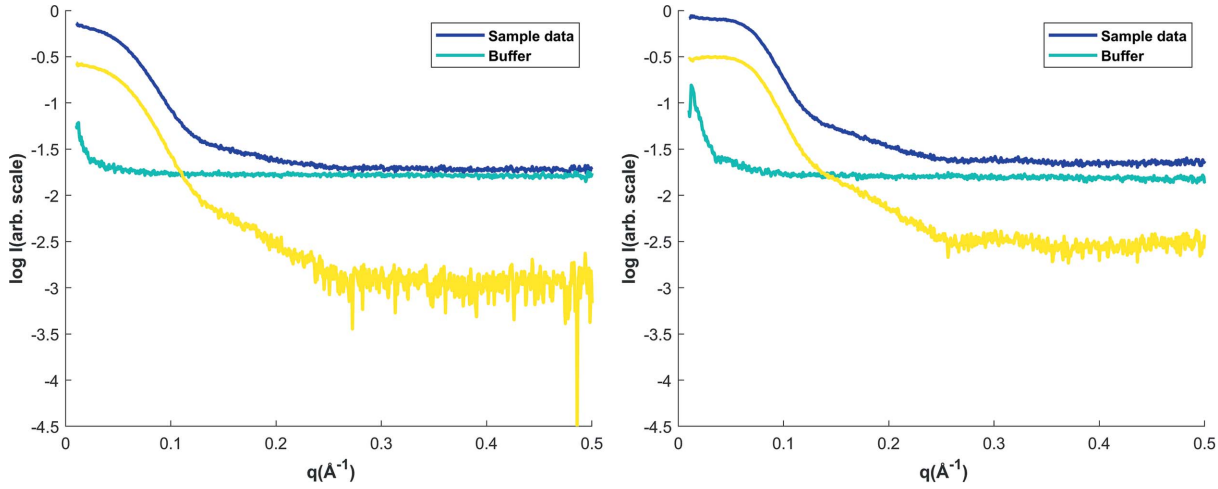

Figure 3
Raw data for 20 mg ml^{-1} rHSA (in 145 m*M* NaCl, 8 m*M* octanoate, 0.05 mg ml^{-1} polysorbate 80). Buffer and subtracted data for the first (*a*) and last (*b*) measurement of the experiment. The data have been normalized by concentration.

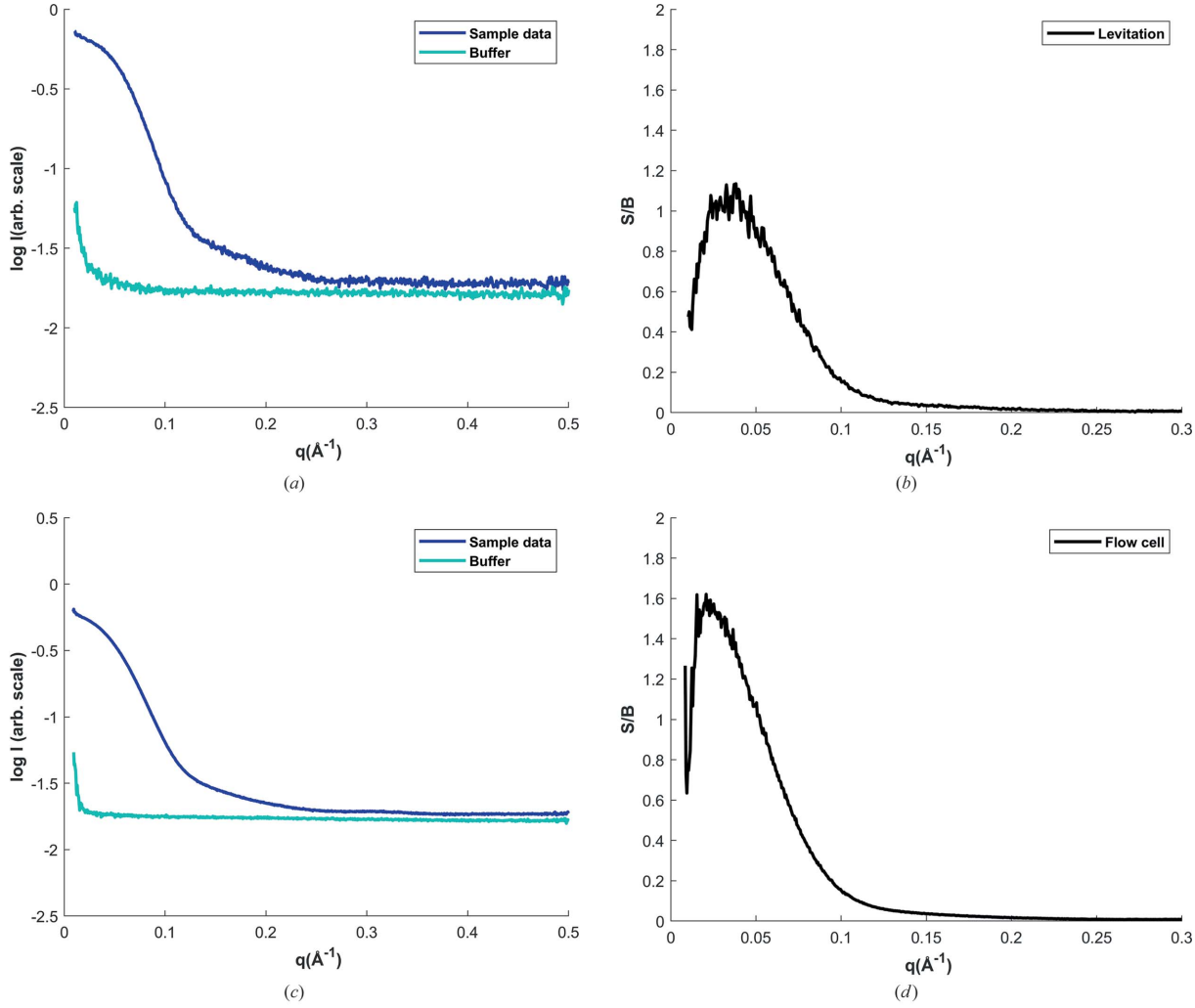

Figure 4
(*a*, *b*) 20 mg ml^{-1} first measurement droplet. (*c*, *d*) 20 mg ml^{-1} flow cell. (*a*, *c*) Measured sample (dark blue) and buffer scattering (turquoise). (*b*, *d*) S/B ratio as defined in equation (8). Buffer composition: 145 m*M* NaCl, 8 m*M* octanoate, 0.05 mg ml^{-1} polysorbate 80.

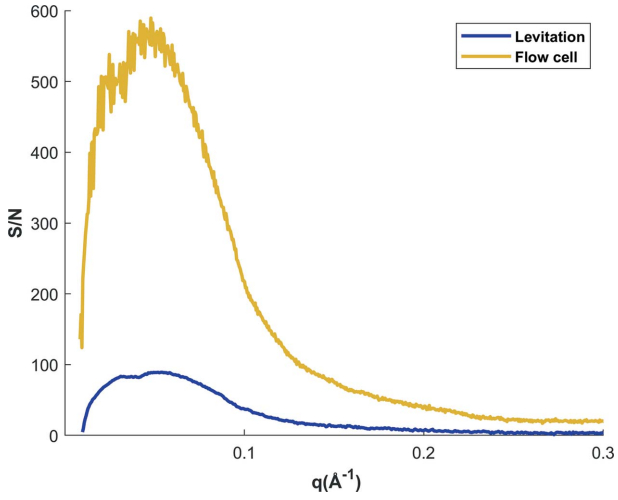

Figure 5
$I/\sigma I$ for 20 mg ml^{-1} rHSA in 145 mM NaCl, 8 mM octanoate, 0.05 mg ml^{-1} polysorbate 80 buffer solution for both setups.

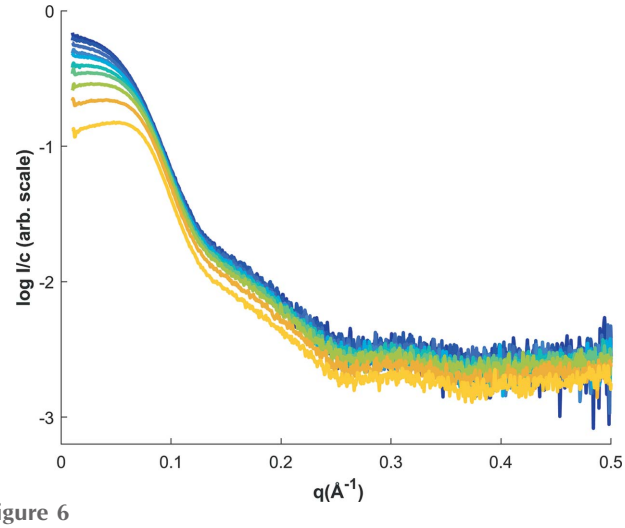

Figure 6
Data measured from one droplet of rHSA with initial concentration of 20 mg ml^{-1}. The curves have been scaled by concentration determined from the droplet volume. The data are not superimposed at high-q, as expected if only the structure factor of the system is varying with concentration.

tering, $I(q)$ and the error associated with it, σI, shows a similar picture, and also indicates that the flow cell data are superior, depicted in Fig. 5.

However, the data from the levitator setup do have a quality making it suitable for data interpretation (and modelling) as shown in the sections below.

3.2. Analysis and scaling of data

When analysing and scaling the data, it was important to pay attention to the experimental setup. Plotting $I(q)/c$ would give superimposed scattering curves in a conventional flow-through cell setup, where the difference between them would only be due to the contribution from the structure factor. This is not the case when we measure in an acoustic levitated droplet containing buffer components. The buffer components are concentrated together with the protein. This means that the buffer is changing with each measurement and therefore the contrast decreases. The effect is visible in Fig. 6, and discussed in detail in the following.

The scattered intensity is proportional to the square of the density contrast ($\Delta\rho$) between protein and solvent (Jacques & Trewhella, 2010),

$$I(q) \propto \Delta\rho^2. \tag{9}$$

Upon evaporation in the droplet, the buffer and salt concentrations are increasing together with the protein concentration. This means that the density contrast $\Delta\rho$ and thereby also the intensity, $I(q)$, will decrease. This effect is estimated in a system containing only NaCl and protein, and shown in Fig. 7. Here, density values for NaCl solutions, found in the literature (Perry & Green, 1997), were used to estimate $I(0)$, shown with red circles and calculated from

$$I(0) = \frac{\Delta\rho_{\rm M}^2\,{\rm MM}\,c}{N_{\rm A}}, \tag{10}$$

where $\Delta\rho_{\rm M}$ is the change in scattering length per mass, $\Delta\rho_{\rm M} = (\rho_{\rm M,protein} - \rho_{\rm solvent})\,\bar{\upsilon} r_0$, where $\bar{\upsilon}$ is the protein partial specific volume (set to 0.7425 cm^3 g^{-1}) and r_0 is the scattering length of an electron (Mylonas & Svergun, 2007). $\rho_{\rm M,protein}$ of rHSA was estimated to be 428 electrons nm^{-3}, as described by Sarachan *et al.* (2013). $N_{\rm A}$ is Avogrado's constant and MM is the molecular mass.

Values of $I(0)$ estimated from the experimental SAXS curves from a droplet of rHSA, 20 mg ml^{-1}, have been plotted alongside in yellow. The experimental decrease we observe in $I(0)$ is more abrupt, probably due to the fact that both polysorbate 80 and octanoate also become more concentrated and thereby add to the decrease in intensity of the scattering curves as observed in Fig. 3.

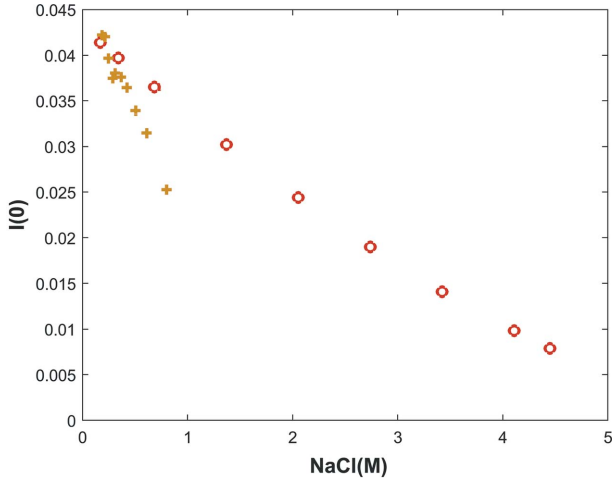

Figure 7
$I(0)$ for 1 mg ml^{-1} HSA as a function of NaCl concentration. For HSA, the scattering length density is set to 428 electrons nm^{-3}. The densities for NaCl at different concentrations were taken from Perry & Green (1997), which in turn were used to calculate $I(0)$, shown as red circles. Normalized $I(0)$ values from the experimental SAXS curves from an rHSA droplet in this study are shown as orange crosses.

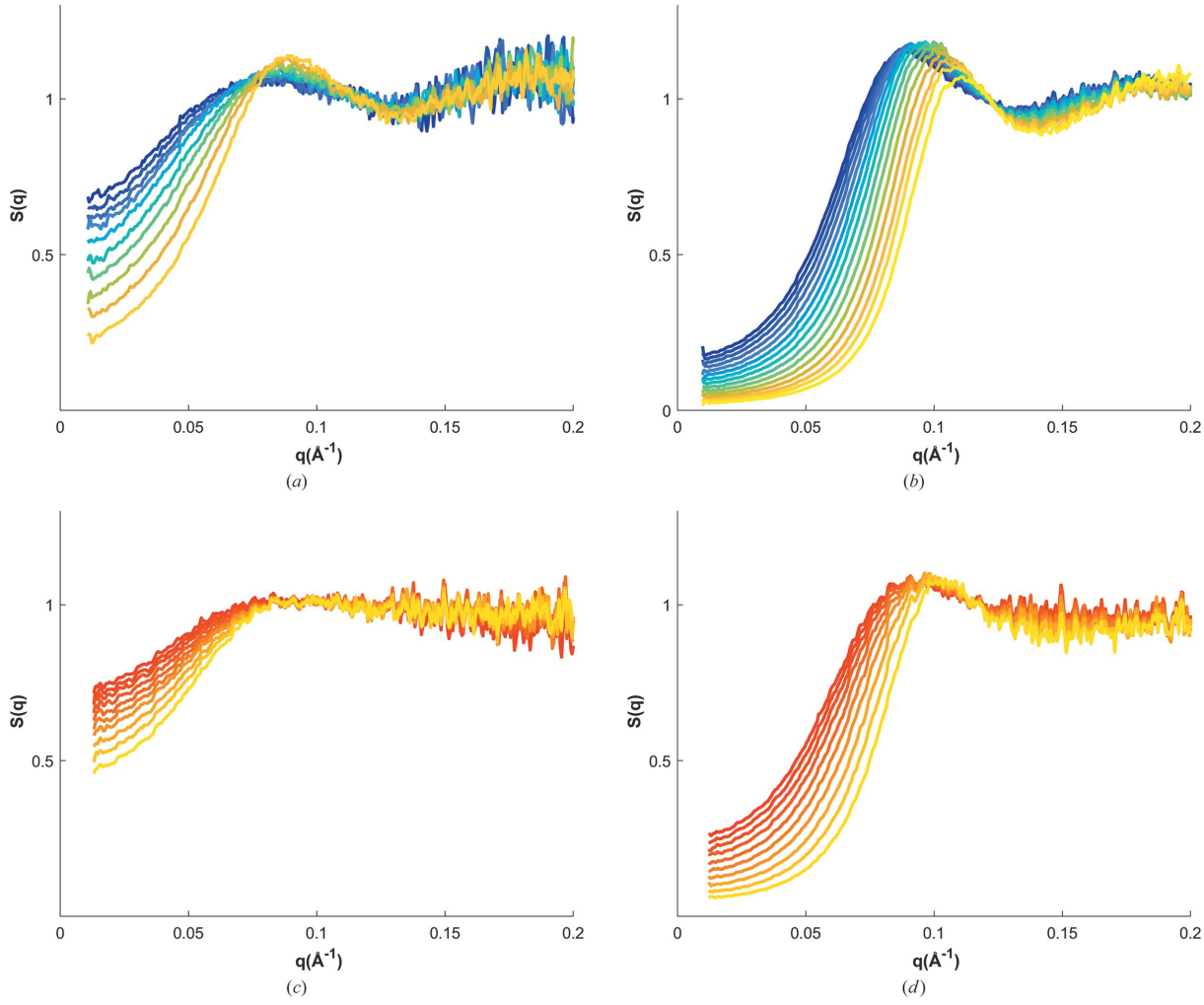

Figure 8
Structure factors derived from initial rHSA concentration of (*a*, *c*) 20 mg ml^{-1} and (*b*, *d*) 100 mg ml^{-1}. (*a*, *b*) In 145 m*M* NaCl, 8 m*M* octanoate and 0.05 mg ml^{-1} polysorbate 80, and (*c*, *d*) in 25 m*M* NaH_2PO_4, 215 m*M* NaCl. Each set of curves correspond to one droplet experiment. The concentration range measured is detailed in each plot.

3.3. Monitoring molecular interactions at high concentrations

An important reason to derive the structure factors on high concentrated solution samples could be to assess the quantity $1/S(q = 0)$, which is related to the second virial coefficient, B_{22}, through $S(0)^{-1} = (1/M_w) + 2B_{22}c$. This in turn describes the overall nature of the interaction of the molecules in the given sample. Structure factors, $S(q)$, for the experiments given in Table 2 are presented in Fig. 8.

From the structure factors shown in Fig. 8, $1/S(0)$ (extracted by extrapolation of the data to $q = 0$) can be derived. In Fig. 9, $1/S(0)$ is plotted together with data derived from previous studies (Sønderby *et al.*, 2018). $1/S(0)$ increases with increasing protein concentration and decreases with increasing salt until all charges have been completely screened.

The agreement between the measurements is good and the levitation experiments provide the same result on a faster time scale, consuming only a small amount of protein. One levitation experiment covers a wide range of protein and salt

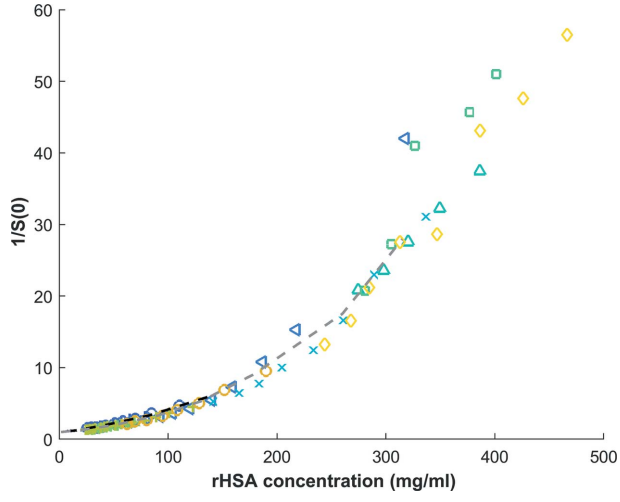

Figure 9
$1/S(0)$ versus concentration for all rHSA samples acoustically levitated, compared with $1/S(0)$ derived from data given by Sønderby *et al.* (2018) (dashed lines).

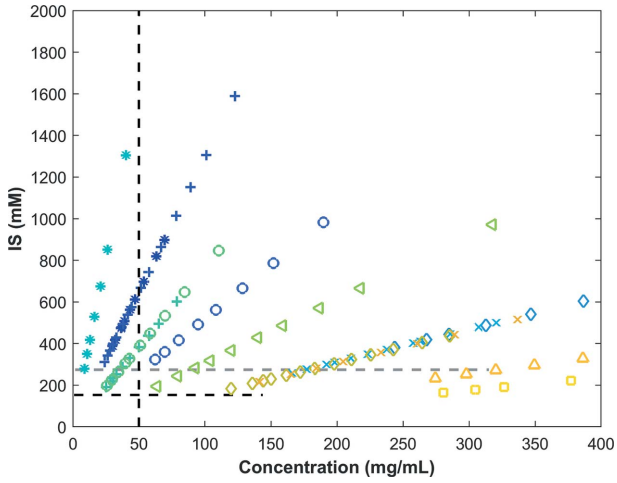

Figure 10
Ionic strength, IS, versus rHSA concentration sample map. The dashed lines represent 26 flow-cell measurements (Sønderby *et al.*, 2018).

concentrations within 10 min. As an example, one droplet of 20 mg ml^{-1} rHSA was concentrated from 20 to 69 mg ml^{-1} covering an ionic strength range of 259–900 m*M*. The amount of protein used for this experiment is 20 mg ml^{-1} × 3 µL = 60 µg. A droplet of 100 mg ml^{-1} would cover 100–350 mg ml^{-1} and use 300 µg protein. In a flow-cell experiment using 30 µL per sample in a series where 1, 2, 5, 10, 20, 50, 100, 150, 200 and 250 mg ml^{-1} are measured, approximately 24 mg of protein is used. These calculations do not take into account the dead volumes, failed experiments, protein lost in preparation, *etc*.

An overview of the sample space covered in this study is plotted in Fig. 10; the dotted lines demonstrate the protein concentration and ionic strength map normally covered in an experiment series.

The highest protein concentration reached practically was approximately 400 mg ml^{-1}. This is far beyond the concentrations that can normally be handled in a conventional bioSAXS setup, typically up to 150 mg ml^{-1}, although occasionally higher concentrations have been measured (Sønderby *et al.*, 2018; Zhang *et al.*, 2007).

In practice, the droplets could be concentrated further, but, as the droplet size eventually becomes comparable with the beam size, then spurious scattering and reflection on the droplet surface prevent further analysis of the data (see Fig. S3). With the new highly focused beamlines with small beam size this issue will probably be less relevant and one could imagine that, by adding a humidity control to the system, to delay the droplet evaporation, and a drop dispenser, to reproducibly levitate the samples, the setup could be standardized.

4. Conclusion

We have demonstrated that by using a levitated droplet setup and an appropriate data correction routine it is possible to obtain high-quality protein solution data in a reproducible way and using only small amounts of sample, *i.e.* down to 3 µL per measurements. Using this method, it is possible to achieve concentrations that would not be accessible in other ways (for example, conventional capillary-based flow-through cells). Used in routine measurements (for example, industrial applications), the benefits in protein cost and time saving will be enormous. The protein concentration and ionic strength parameter space diagram may be covered easily and the amount of protein sample is significantly reduced (by a factor of 100 in this work).

The methods may also be relevant for protein samples that cannot be obtained in high enough concentrations to produce good quality scattering data for structure factor determination. In the present setup, increases in concentration up to a factor of five are easily obtained after approximately 10 min under levitation, depending on the start concentration and buffer conditions.

Acknowledgements

The MAX IV synchrotron is acknowledged for providing beam time for the project. Albumedix Ltd is acknowledged for kindly providing the albumin samples.

Funding information

The following funding is acknowledged: Danish Agency for Science, Technology, and Innovation for funding the instrument center DanScatt; EU Interreg project ÖKS (40789) for financial support to PS.

References

Agthe, M., Plivelic, T. S., Labrador, A., Bergström, L. & Salazar-Alvarez, G. (2016). *Nano Lett.* **16**, 6838–6843.
Ashiotis, G., Deschildre, A., Nawaz, Z., Wright, J. P., Karkoulis, D., Picca, F. E. & Kieffer, J. (2015). *J. Appl. Cryst.* **48**, 510–519.
Cavalcanti, L. P., Torriani, I. L., Plivelic, T. S., Oliveira, C. L. P., Kellermann, G. & Neuenschwander, R. (2004). *Rev. Sci. Instrum.* **75**, 4541–4546.
Cristiglio, V., Grillo, I., Fomina, M., Wien, F., Shalaev, E., Novikov, A., Brassamin, S., RéFrégiers, M., Pérez, J. & Hennet, L. (2017). *Biochim. Biophys. Acta*, **1861**, 3693–3699.
Delissen, F., Leiterer, J., Bienert, R., Emmerling, F. & Thünemann, A. F. (2008). *Anal. Bioanal. Chem.* **392**, 161–165.
Dubuisson, J.-M., Decamps, T. & Vachette, P. (1997). *J. Appl. Cryst.* **30**, 49–54.
Foresti, D., Nabavi, M., Klingauf, M., Ferrari, A. & Poulikakos, D. (2013). *Proc. Natl Acad. Sci.* **110**, 12549–12554.
Frohn, A. & Roth, N. (2000). *Dynamics of Droplets*, edited by A. Frohn & N. Roth. New York: Springer.
Gasteiger, E., Hoogland, C., Gattiker, A., Duvaud, S., Wilkins, M. R., Appel, R. D. & Bairoch, A. (2005). *The Proteomics Protocols Handbook.*, edited by J. M. Walker, pp. 571–607. Totowa: Humana Press.
Jacques, D. & Trewhella, J. (2010). *Protein Sci.* **19**, 642–657.
Konarev, P. V., Petoukhov, M. V., Volkov, V. V. & Svergun, D. I. (2006). *J. Appl. Cryst.* **39**, 277–286.
Konarev, P. V., Volkov, V. V., Sokolova, A. V., Koch, M. H. J. & Svergun, D. I. (2003). *J. Appl. Cryst.* **36**, 1277–1282.
Labrador, A., Cerenius, Y., Svensson, C., Theodor, K. & Plivelic, T. (2013). *J. Phys. Conf. Ser.* **425**, 072019.
Leiterer, J., Delissen, F., Emmerling, F., Thünemann, A. F. & Panne, U. (2008*b*). *Anal. Bioanal. Chem.* **391**, 1221–1228.
Leiterer, J., Grabolle, M., Rurack, K., Resch-Genger, U., Ziegler, J., Nann, T. & Panne, U. (2008*a*). *Ann. NY Acad. Sci.* **1130**, 78–84.

Lü, Y. J., Xie, W. J. & Wei, B. (2005). *Appl. Phys. Lett.* **87**, 184107.
Meisburger, S. P., Warkentin, M., Chen, H., Hopkins, J. B., Gillilan, R. E., Pollack, L. & Thorne, R. E. (2013). *Biophys. J.* **104**, 227–236.
Mylonas, E. & Svergun, D. I. (2007). *J. Appl. Cryst.* **40**, s245–s249.
Orthaber, D., Bergmann, A. & Glatter, O. (2000). *J. Appl. Cryst.* **33**, 218–225.
Pellicane, G. & Cavero, M. (2013). *J. Chem. Phys.* **138**, 115103.
Perry, R. H. & Green, D. W. (1997). *Perry's Chemical Engineers' Handbook*, 7th ed., edited R. H. Perry & D. W. Green, pp. 2–105. McGraw-Hill.
Sadek, C., Schuck, P., Fallourd, Y., Pradeau, N., Le Floch-Fouéré, C., Jeantet, R. & Jeantet, R. (2015). *Dairy Sci. Technol.* **95**, 771–794.
Saluja, A. & Kalonia, D. S. (2008). *Int. J. Pharm.* **358**, 1–15.
Sarachan, K. L., Curtis, J. E. & Krueger, S. (2013). *J. Appl. Cryst.* **46**, 1889–1893.
Schiffter, H. & Lee, G. (2007*a*). *J. Pharm. Sci.* **96**, 2274–2283.
Schiffter, H. & Lee, G. (2007*b*). *J. Pharm. Sci.* **96**, 2284–2295.
Shire, S. J., Shahrokh, Z. & Liu, J. (2004). *J. Pharm. Sci.* **93**, 1390–1402.
Sønderby, P., Bukrinski, J. T., Hebditch, M., Peters, G. H. J., Curtis, R. A. & Harris, P. (2018). *ACS Omega*, **3**, 16105–16117.
Tardieu, A., Laporte, D. & Delaye, M. (1987). *J. Phys. Fr.* **48**, 1207–1215.
Tsujino, S. & Tomizaki, T. (2016). *Sci. Rep.* **6**, 25558.
Xie, W. J., Cao, C. D., Lü, Y. J. & Wei, B. (2002). *Phys. Rev. Lett.* **89**, 104304.
Zhang, F., Skoda, M. W., Jacobs, R. M. J., Martin, R., Martin, C. M. & Schreiber, F. (2007). *J. Phys. Chem. B*, **111**, 251–259.